JOURNAL OF APPLIED ELECTROCHEMISTRY 26 (1996) 683–688

Electrochemical properties of $Ti/SnO_2–Sb_2O_5$ electrodes prepared by the spray pyrolysis technique

B. CORREA-LOZANO, CH. COMNINELLIS*, A. DE BATTISTI‡

Institute of Chemical Engineering, Swiss Federal Institute of Technology, CH-1015 Lausanne, Switzerland

Received 27 February 1995; revised 10 January 1996

Cyclic voltammetry for the ferri-ferrocyanide redox couple has been used to study the $Ti/SnO_2–Sb_2O_5$ electrode prepared by spray-pyrolysis under different conditions. The obtained results shows that increasing the preparation temperature and the duration of coating deposition results in a decrease of i_p and an increase of ΔE_p for the ferri-ferrocyanide couple. This deviation from reversibility has been attributed to the formation of a titanium oxide layer at the Ti/coating interface. Concerning oxygen evolution at the $Ti/SnO_2–Sb_2O_5$ anodes, a mechanism is proposed in which water is discharged at the anode forming hydroxyl radicals which are further oxidized to form dioxygen. Finally, a generalized mechanism for oxygen evolution at oxide electrodes has been proposed.

1. Introduction

The literature on dimensionally stable anodes (DSA®) [1, 2] shows that the nature of the oxide coating strongly influences their electrochemical behaviour. While electrodes based on RuO_2 and TiO_2 are widely used in chlor-alkali cells, electrodes based on IrO_2 and Ta_2O_5 can be used for oxygen evolution in sulfuric acid media [3, 4]. The case of SnO_2 in this context is quite interesting, its role ranging between that of minor component of some DSA® materials and that of main component in $SnO_2–Sb_2O_5$ film electrodes, of interest in electrochemical combustion of organics [5–10].

Some aspects of the electrochemical behaviour of $Ti/SnO_2–Sb_2O_5$ electrodes have been discussed earlier [11, 12]. Preparation of these electrode materials and physicochemical and electrochemical properties have been discussed in relation with their application for the electrochemical combustion of organic pollutants in aquatic media [5–10]. Further detailed treatment of the preparation problems, with special reference to spray pyrolysis, have been given [13, 14]. Correlations between preparation parameters and physicochemical properties, have been described too [15].

In the present paper an electrochemical study of $Ti/SnO_2–Sb_2O_5$ electrodes has been carried out. The formation of titanium oxide at the Ti/coating interface during electrode preparation has been followed by cyclic voltammetry using the $[Fe(CN)_6]^{3-}/[Fe(CN)_6]^{4-}$ redox couple. The mechanism of oxygen evolution has been studied by cyclic voltammetry and by steady state polarization measurements.

2. Experimental details

The cyclic voltammetry experiments were carried out with an EG&G PAR potentiostat–galvanostat (model 362). A three-electrode cell was used. The $Ti/SnO_2–Sb_2O_5$ electrodes ($6\,cm^2$) were prepared on titanium base metal by spray pyrolysis; the composition of the spray solution was 10 g $SnCl_4 \cdot 5H_2O$, 0.2 g $SbCl_3$ in 100 ml of ethanol–HCl mixture. Unless otherwise stated, the mixed oxide loading amounted to $25\,g\,m^{-2}$, corresponding to a thickness of about $4\,\mu m$. Details of the preparation have been given elsewhere [13, 14]. The counterelectrode consisted of two interconnected platinum spirals (total surface $25\,cm^2$) positioned in front of the two faces of the working electrode, respectively. An $Hg/Hg_2SO_4/K_2SO_4$ (sat.) electrode (Metrohm, model 6.0703.100) was used as reference. The solution temperature was maintained at 25 °C.

Quasisteady state polarization curves with *iR* drop correction were carried out using the same potentiostat–galvanostat unit and the same cell as used for the cyclic voltammetry experiments, with one reference electrode more. Due to the possibility of significant ohmic drops at the Ti/oxide interface, ohmic drop correction becomes particularly important in this case. This was achieved using the arrangement shown in Fig. 1. The current interruption switch was custom built. It was based on two timing units and two MOS switches (model AQV-201).

The response delay of the switches was less than 80 ms. One of the switches was connected to the anode, the other to the cathode. One of the two

* To whom correspondence should be addressed.
‡ Permanent address: Department of Chemistry of the University of Ferrara, Italy.

0021-891X

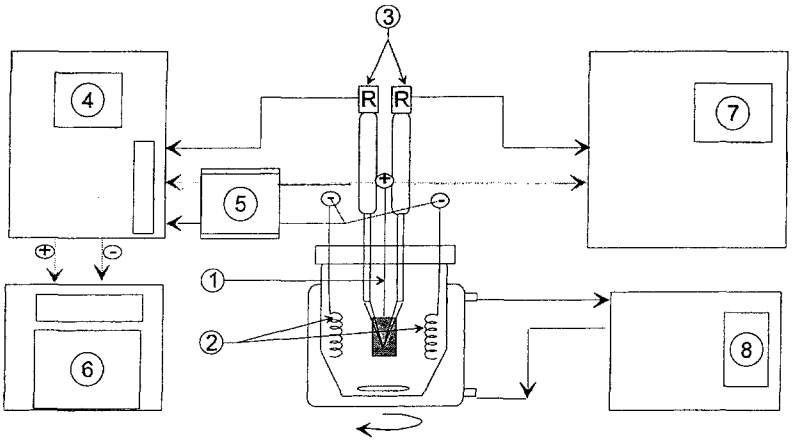

Fig. 1. Scheme of the equipment used for the measurement of current/potential curves. (1) Anode (WE); (2) Pt cathodes (CE); (3) reference electrodes; (4) potentiostat–galvanostat; (5) current interruption block; (6) X–Y recorder; (7) digital oscilloscope; (8) thermostatic unit.

clocks measured the real duration of the measurement, the other checked the duration of the current interruption. The change with time of the potential of the potential difference between working electrode and the second reference, after current interruption, was followed by a memory storage oscilloscope (Gould, model 1602 DSO).

3. Results and discussion

3.1. *Voltammetric behaviour of the* $[Fe(CN)_6]^{3-}/[Fe(CN)_6]^{4-}$ redox couple

The behaviour of the $[Fe(CN)_6]^{3-}/[Fe(CN)_6]^{4-}$ redox couple, involving only outer-sphere electron transfer, was studied at $SnO_2-Sb_2O_5$ films supported on titanium, in order to investigate the influence of preparation variables on the Ti/coating interface.

In Fig. 2, cyclic voltammograms of the ferriferrocyanide couple are compared for $Ti/SnO_2-Sb_2O_5$ electrodes prepared at different temperatures, between 400 and 550 °C. With increasing preparation temperature, a decrease in the peak current density i_p, and an increase in the potential difference between anodic and cathodic peak, ΔE_p can be observed. In Fig. 3, the dependence of i_p on $v^{1/2}$, is shown. A good linearity is observed for the electrode prepared at 450 °C (curve (a)) over the whole v range. For the sample prepared at 550 °C (curve (b)) this is observed only below $0.010\,V\,s^{-1}$. From the slope of the $i_p/v^{1/2}$ plot in Fig. 3 (curve (a)), a value of $1.2 \times 10^{-9}\,m^2\,s^{-1}$ could be calculated for the diffusion coefficient of the electroactive species, close to literature value [16].

The influence of the duration of coating deposition on i_p and ΔE_p is shown in Fig. 4, a decrease of i_p (curve (a)) an increase of ΔE_p (curve (b)) is observed, with increasing the duration of coating deposition.

This deviation from reversibility of the ferri-ferrocyanide couple with increasing preparation temperature and duration of deposition, has been attributed to the formation of a titanium oxide layer at the Ti/coating interface.

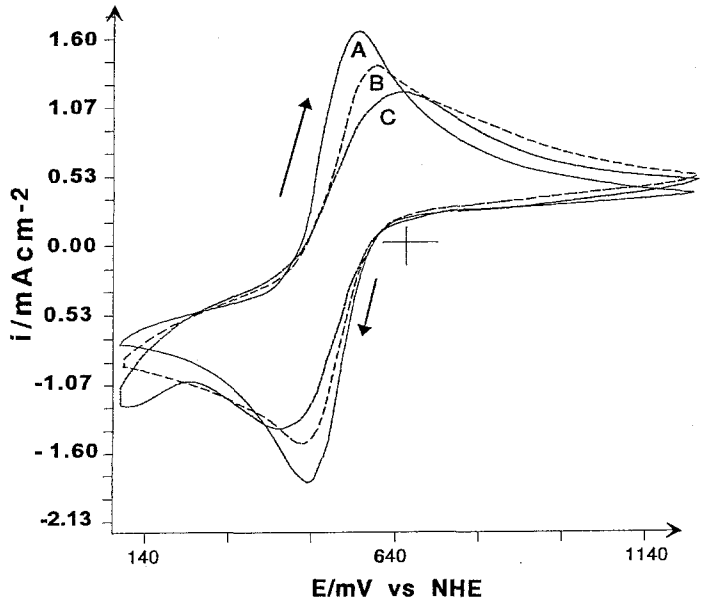

Fig. 2. Cyclic voltammograms of the $[Fe(CN)_6]^{3-}/[Fe(CN)_6]^{4-}$ redox couple at $Ti/SnO_2-Sb_2O_5$ electrodes prepared at different temperatures: (a) 400 °C; (b) 500 °C; (c) 550 °C. The concentration of ferri- and ferrocyanide was 10 mM and the supporting electrolyte was 0.1 M H_2SO_4 + 0.5 M Na_2SO_4. $v = 20\,mV\,s^{-1}$ and $T = 25$ °C.

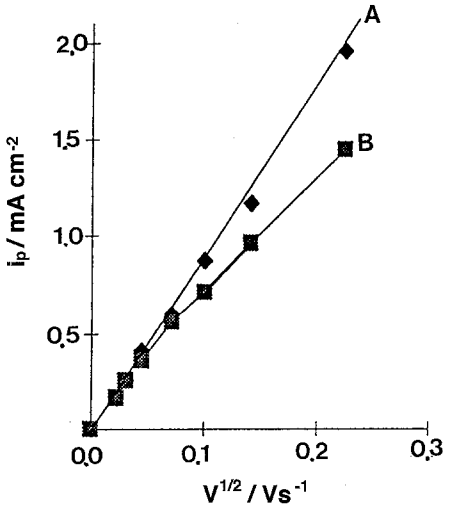

Fig. 3. Dependence of the peak current density, i_p, on the square root of the potential scan rate, $v^{1/2}$, for the ferri-ferrocyanide redox couple at $Ti/SnO_2-Sb_2O_5$ electrodes prepared at different temperatures: (a) 450 °C; (b) 550 °C. Electrolyte as in Fig. 2. $T = 25$ °C.

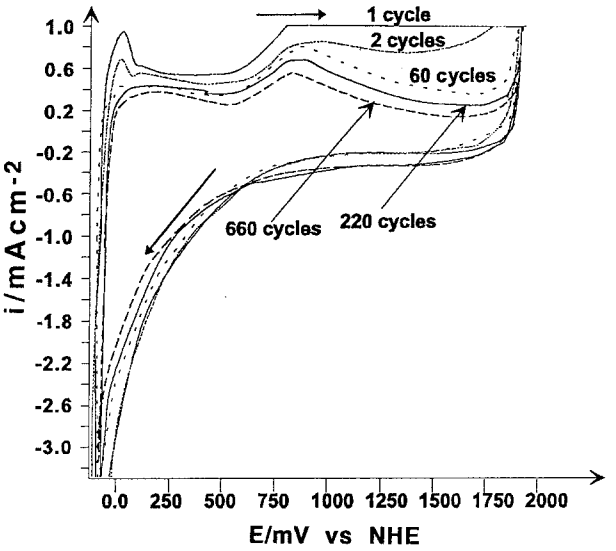

Fig. 5. Shape modification of cyclic voltammograms for a $Ti/SnO_2-Sb_2O_5$ electrode with increasing the number of polarization cycles. $v = 20$ mV s^{-1}. Electrolyte: 0.5 M H_2SO_4; $T = 25$ °C.

Minimization of the Ti/coating interface can be achieved by reducing deposition temperature. However, need for large thickness and good electrical conductivity of the deposit restrict the choice of the deposition conditions, the value of 550 °C adopted in this work being most probably the best one. The only way to minimize the oxidation of titanium substrate is, therefore, to reduce the deposition time, by increasing the solution flow [14]. At 550 °C the $Ti/SnO_2-Sb_2O_5$ film growth rate can be led to a maximum of about 0.8 μm min^{-1}, which would allow attainment of 4–5 μm thicknesses with a spraying time of 7–8 min. Improvement of film adhesion and stability of the Ti/coating interface, however, requires synthesis of convenient interlayers prior to the $SnO_2-Sb_2O_5$ film deposition [22].

3.2. *Cyclic voltammetry in 0.5 M H_2SO_4*

In Fig. 5, cyclic voltammograms obtained in 0.5 M H_2SO_4, at 25 °C are shown. In the first two cycles, important anodic phenomena, probably bound to rearrangement of the oxide/solution interface and oxidation of impurities take place. After 60 cycles the shape of the voltammogram remains more or less constant, with only smaller changes with increasing the number of cycles.

The anodic part of the voltammogram exhibits a well defined peak, already at the second cycle (Fig. 5), whose maximum is at about 0.90 V vs NHE. No corresponding peak is found in the cathodic voltammogram, in which, however, a monotonous increase of current takes place, starting from about 0.70 V, followed by hydrogen evolution reaction itself. Another smaller anodic peak is also evident at 0.0 V, probably due to oxidation of adsorbed hydrogen.

To verify the reproducibility of the voltammograms, experiments were also carried out on electrochemically preconditioned electrodes. Preconditioning consisted in polarizing the electrodes for two hours under an anodic current of 50 mA cm^{-2}. A comparison between the behaviour of as-prepared (second cycle) and preconditioned electrodes is given in Fig. 6.

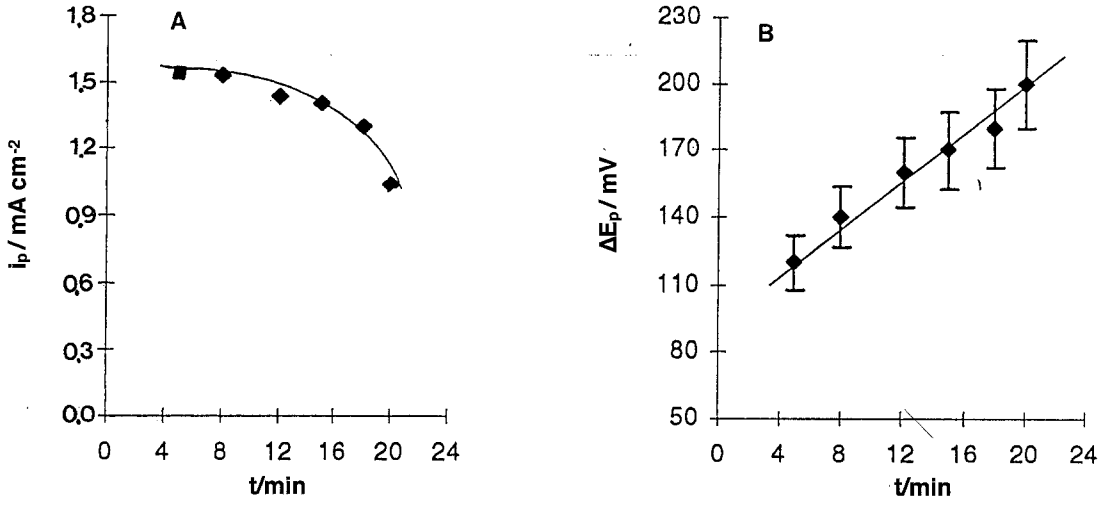

Fig. 4. Dependence of i_p and ΔE_p, on the duration of the thermal treatment (curves (a) and (b), respectively). The final oxide loading was in any case 25 g cm^{-2}. Electrolyte as in Fig. 2. $v = 20$ mV s^{-1}. $T = 25$ °C.

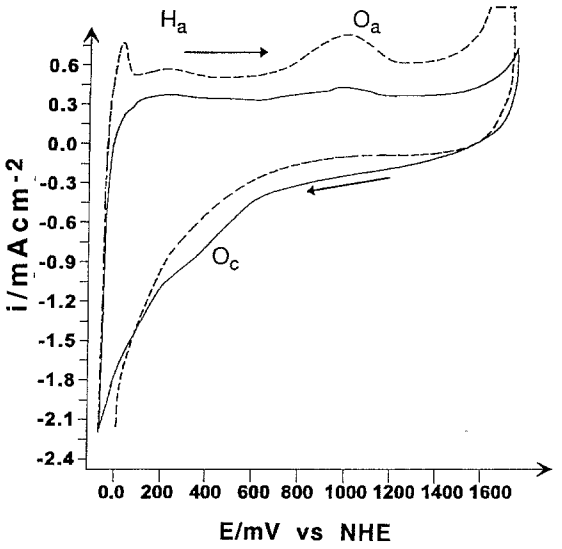

Fig. 6. Cyclic voltammogram for an 'as prepared' electrode (- - - - -) and for a preconditioned electrode (——) (anodic polarization at 50 mA cm^{-2} for 2 h). Electrolyte as in Fig. 5. $v = 20$ mV s^{-1}. $T = 25$ °C.

For the latter only a trace of the anodic peak O_a, remains, and no other anodic signal is visible. A cathodic peak, O_c, appears, around 0.45 V. The reproducibility of the voltammograms for the activated electrode was found to be quite good. Apparently, the anodic pre-polarization also involves a significant deactivation of the electrode for the oxygen evolution reaction.

Under the established pre-conditioning the influence of the value of the positive reversal potential E_r on the shape of the voltammograms was investigated. As shown in Fig. 7, with extending the polarization window in the direction of positive potentials, the O_c peak current increases. The increase becomes more significant for $E_r > 1.50$ V (Fig. 8). The formation of the intermediate whose reduction gives origin to O_c, evidently occurs only above a given anodic potential. The absence of a corresponding anodic

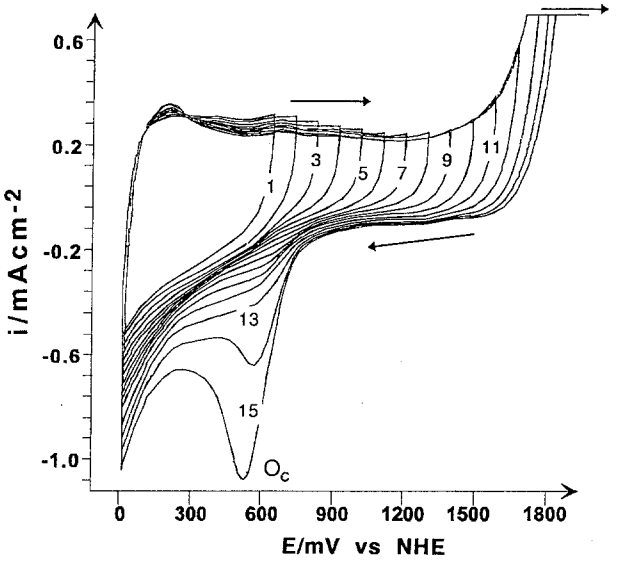

Fig. 7. Change of the cyclic voltammogram for a preconditioned Ti/SnO_2–Sb_2O_5 electrode, with increasing the positive reversal potential E_r by 0.1 V intervals (curves 1–15). Electrode as in Fig. 5. $v = 20$ mV s^{-1}, $T = 25$ °C.

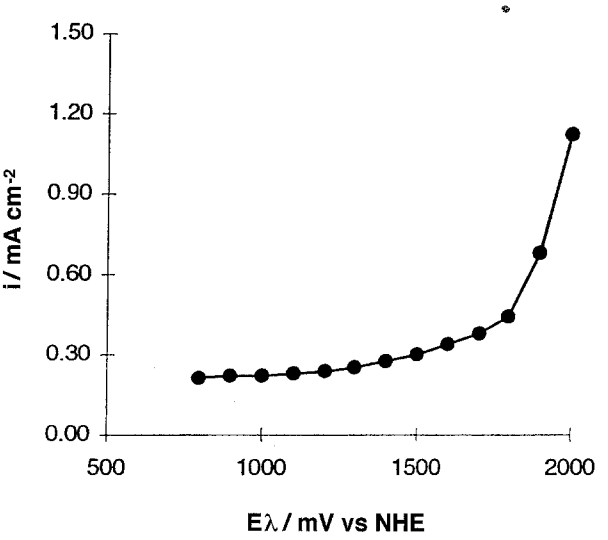

Fig. 8. Dependence of i_p for the cathodic peak O_c on the value of the positive reversal potential, E_r (see Fig. 7).

signal, which most probably is covered by the oxygen evolution current, points to large irreversibility of the solid state redox process.

In 1 M NaOH the voltammograms become featureless, as shown in Fig. 9. Although most probably confined to the electrode surface, the redox phenomena responsible for the peaks in acidic medium, involve the proton as one of the reactants, as in the case of other oxide electrodes [17–19]. In alkaline media the extension of the potential scan range does not modify the shape of the voltammograms.

In Fig. 10(a) and (b) SEM images of an as-prepared electrode surface (a) and after 800 cycles (b) in 0.5 M H_2SO_4 are shown. Large crystallites of which the oxide films consist, undergo probably extensive reconstruction under cyclic electrochemical polarization.

The initial slow decrease of voltammetric currents with increasing the number of cycles and the concomitant decrease in activity towards the oxygen evolution reaction (Fig. 5) can be explained considering that a certain degree of non-stoichiometry is present

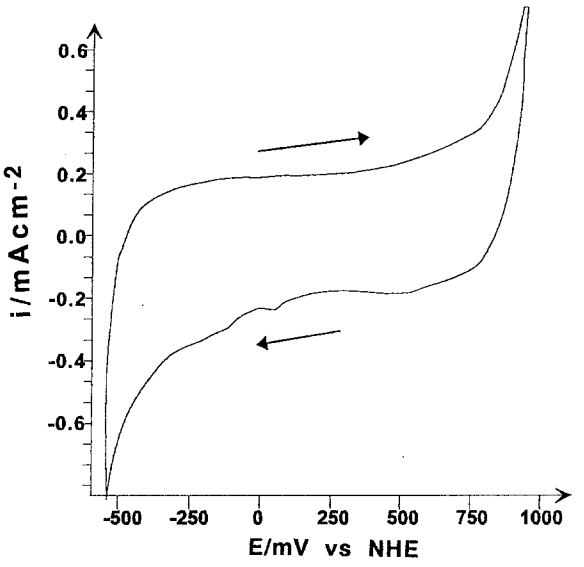

Fig. 9. Cyclic voltammogram of a Ti/SnO_2–Sb_2O_5 electrode in alkaline solution (1 M NaOH). $v = 20$ mV s^{-1}. $T = 25$ °C.

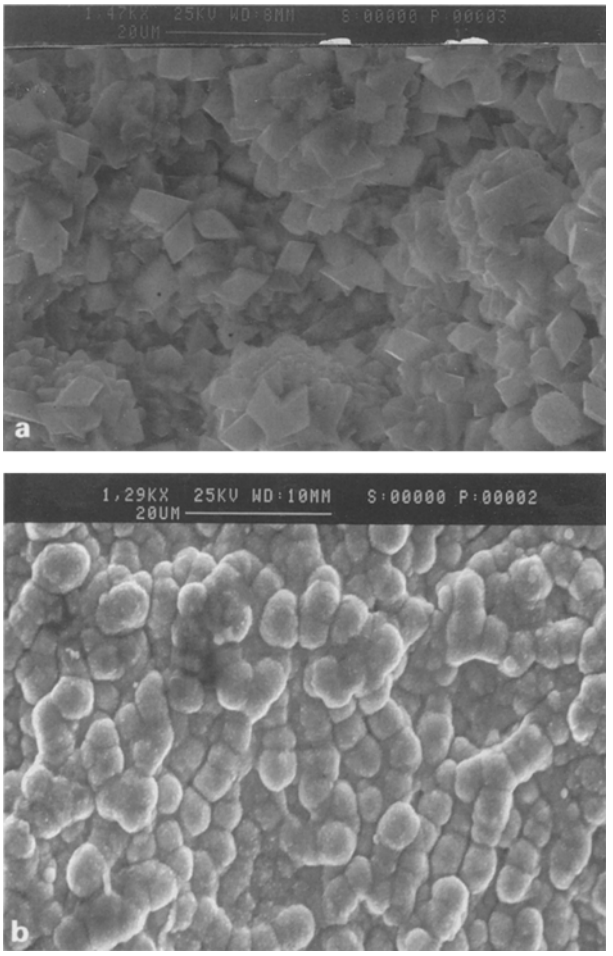

Fig. 10. Effect of potential cycling between −0.050 and 1.950 V vs NHE on the surface morphology of the $Ti/SnO_2-Sb_2O_5$ electrode. SEM image, of an 'as prepared' electrode (a), and after 800 polarization cycles. (b) Electrolyte: 0.5 M H_2SO_4. $T = 25\,°C$.

in as-prepared SnO_2 films [20, 21]. This initial defectivity involves a larger concentration of catalytically active sites, where the reaction:

$$SnO_{(2-x)} + H_2O \longrightarrow SnO_{(2-x)}(^{\bullet}OH) + H^+ + e^- \quad (1)$$

takes place, with formation of adsorbed hydroxyl radicals, $^{\bullet}OH$. A further oxidation may take place, with an increase in oxygen stoichiometry, which, however, at this stage is still below 2 (Equation 2):

$$SnO_{(2-x)}(^{\bullet}OH) \longrightarrow SnO_{(2-x+y)} + yH^+ + ye^- \quad (2)$$

From the decomposition of the species $SnO_{(2-x+y)}$ oxygen can be evolved, with regeneration of $SnO_{(2-x)}$ (Equation 3):

$$SnO_{(2-x+y)} \longrightarrow SnO_{(2-x)} + 1/2\,yO_2 \quad (3)$$

Under anodic polarization and/or cycling between hydrogen and oxygen evolution reaction, reconstruction of the film surface occurs, with loss of defectivity. The oxygen evolution reaction can then occur through the step:

$$SnO_2(^{\bullet}OH) \longrightarrow SnO_2 + 1/2\,O_2 + H^+ + e^- \quad (4)$$

The role played by the anodic preconditioning could then be the progressive increase of the y value towards x.

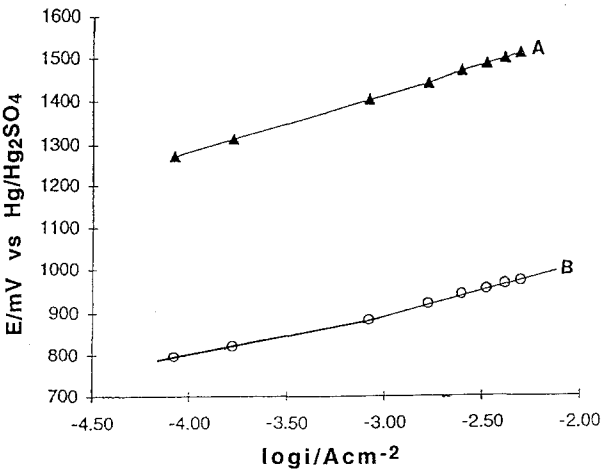

Fig. 11. Tafel plots for oxygen evolution reaction at a $Ti/SnO_2-Sb_2O_5$ electrode (a) and at a Ti/IrO_2 electrode (b). Electrolyte: 0.5 M H_2SO_4. $T = 25\,°C$.

3.3. *Oxygen evolution in acidic medium at $Ti/SnO_2-Sb_2O_5$ anodes*

The Tafel plot corrected for ohmic drop, obtained at a preconditioned $Ti/SnO_2-Sb_2O_5$ electrode in 0.5 M H_2SO_4 is shown in Fig. 11. For the sake of comparison results obtained with a Ti/IrO_2 electrode have also been given. Linearity across about two current density decades is observed for the $Ti/SnO_2-Sb_2O_5$ electrode, with a slope of $0.12\,V\,dec^{-1}$. In agreement with the literature a lower slope, $0.070\,V\,dec^{-1}$ is found for the Ti/IrO_2 electrode at lower current densities. The exchange current density is much larger at the Ti/IrO_2 electrode ($i_0 = 10^{-5}\,A\,cm^{-2}$), than at the $Ti/SnO_2-Sb_2O_5$ electrode ($i_0 = 10^{-9}\,A\,cm^{-2}$). Current/potential curves also allowed an estimate of the potential of incipient oxygen evolution. The value was 1.8 V vs NHE in the case of the $Ti/SnO_2-Sb_2O_5$ electrode and 1.35 V vs NHE for the Ti/IrO_2 electrode. The first is quite close to the H_2O_2/H_2O redox potential (Equation 5) and the second approximates that of the IrO_3/IrO_2 redox equilibrium (Equation 6).

$$H_2O_2 + 2H^+ + 2e^- \rightleftharpoons 2H_2O \quad (5)$$

$$IrO_3 + 2H^+ + 2e^- \rightleftharpoons IrO_2 + H_2O \quad (6)$$

on the basis of the above results a generalized mechanism for oxygen evolution at oxide electrodes in acidic media can be proposed, whose scheme is shown in Fig. 12. In the first step adsorbed hydroxyl radicals, $^{\bullet}OH$, are formed:

$$MO_x + H_2O \longrightarrow MO_x(^{\bullet}OH) + H^+ + e^- \quad (7)$$

In the case of 'inert' oxides, where electroactive sites are absent, weakly adsorbed hydroxyl radicals are further oxidized to form dioxygen, by the so called peroxide mechanism:

$$MO_x(^{\bullet}OH) \longrightarrow 1/2\,O_2 + H^+ + e^- + MO_x \quad (8)$$

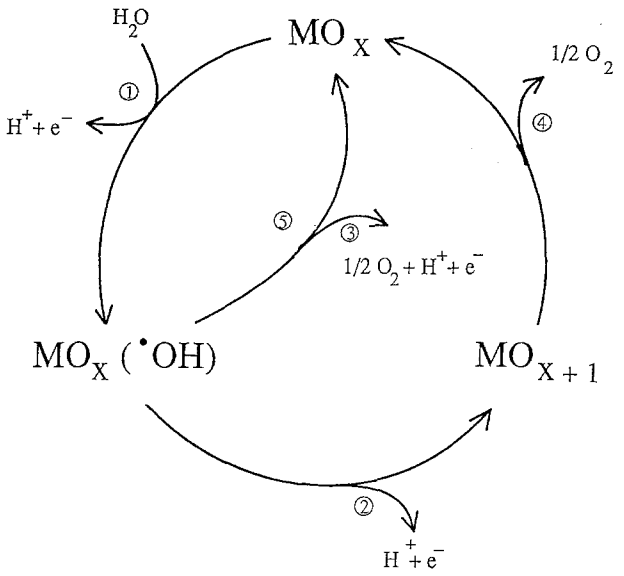

Fig. 12. Mechanism of the oxygen evolution at oxide anodes: (1) formation of $^\bullet OH$ radical by water oxidation; (2) transfer of oxygen from $^\bullet OH$ to the oxide lattice (formation of a higher oxide site); (3) oxygen evolution by electrochemical oxidation of $^\bullet OH$ species; (4) oxygen evolution by chemical decomposition of the higher oxide.

(hydrogen peroxide is probably an intermediate). Apparently at anodically pretreated $Ti/SnO_2-Sb_2O_5$ electrodes the oxygen evolution reaction takes place through steps (7)–(8). In fact, hydroxyl radicals have been detected at the surface of SnO_2 electrodes during water oxidation [9]. The lack of higher oxidation states for the metal ions in the oxide structure involves a lower stability of hydroxyl radicals intermediates, which justifies the high overvoltages of the oxygen evolution reaction at these electrode materials (Fig. 11).

For metal oxides with electroactive sites (typically the noble metal oxides like RuO_2 and IrO_2), which are catalytically active for oxygen evolution reaction, adsorbed hydroxyl radicals can be stabilized by interaction with metal cations in the oxide lattice, causing a formal increase of their oxidation state:

$$MO_x(^\bullet OH) \longrightarrow MO_{x+1} + H^+ + e^- \qquad (9)$$

The decomposition of this unstable species gives origin to dioxygen:

$$MO_{x+1} \longrightarrow MO_x + 1/2\,O_2 \qquad (10)$$

4. Conclusion

The electrochemical study of the $Ti/SnO_2-Sb_2O_5$ electrode prepared by spray-pyrolysis technique has shown that the experimental conditions influence strongly the performance of this electrode. This has been attributed to the formation of a titanium oxide layer at the Ti/coating interface.

A mechanism for oxygen evolution at $Ti/SnO_2-Sb_2O_5$ electrode is proposed in which H_2O is discharged forming $^\bullet OH$ which are further oxidized to dioxygen.

References

[1] Ch. Comninellis and G. P. Vercesi, *J. Appl. Electrochem.* **21** (1991) 335.
[2] Ch. Comninellis and G. P. Vercesi, *ibid.* **21** (1991) 136.
[3] G. P. Vercesi, J. Y. Salamin and Ch. Comninellis, *Electrochim. Acta.* **36** (1991) 991.
[4] G. P. Vercesi, J. Rolewicz, J. Hinden and Ch. Comninellis, *Thermochim. Acta* **176** (1991) 31.
[5] R. Kötz, S. Stucki and B. Carcer, *J. Appl. Electrochem.* **21** (1991) 14.
[6] S. Stucki, R. Kötz, B. Carcer and W. Suter, *ibid.* **21** (1991) 99.
[7] Ch. Comninellis and C. Pulgarin, *ibid.* **23** (1993) 108.
[8] C. Pulgarin, N. Adler, P. Péringer and Ch. Comninellis, *Wat. Res.* **28**(4) (1994) 887.
[9] Ch. Comninellis, *Electrochim. Acta* **39** (1994) 1857.
[10] Ch. Comninellis and A. Nerini, *J. Appl. Electrochem.* **25** (1995) 114.
[11] D. Elliot, D. L. Zellmer and H. A. Laitinen, *J. Electrochem. Soc.* **117** (1970) 1343.
[12] H. A. Laitinen and J. M. Conley, *Analyt. Chem.* **48** (1976) 1224.
[13] B. Correa-Lozano, Ph.D. thesis no. 1297, EPFL, Lausanne (1994).
[14] B. Correa-Lozano, Ch. Comninellis and A. De Battisti, *J. Appl. Electrochem.*, in press.
[15] B. Correa-Lozano, Ch. Comninellis and A. De Battisti, *J. Electrochem. Soc.*, in press.
[16] A. Montillet, J. Comiti and J. Legrand, *J. Appl. Electrochem.* **24** (1994) 384.
[17] L. D. Burke and O. J. Murphy, *J. Electroanal. Chem.* **112** (1980) 39.
[18] S. Trasatti and G. Lodi, *in* 'Electrodes of Conductive Metal Oxides', Part A (edited by S. Trasatti), Elsevier, Amsterdam (1980), p. 301.
[19] D. M. Novak, B. V. Tilac and B. E. Conway, *in* 'Modern Aspects of Electrochem.', vol. 14 (edited by B. E. Conway and J. O'M. Bockris), Plenum, New York (1982) p. 195.
[20] A. Mani, *J. Mater. Sci. Lett.* **10** (1991) 953.
[21] C. M. Freeman and C. R. A. Cutlow, *J. Solid State Chem.* **85** (1990) 65.
[22] B. Correa-Lozano, Ch. Comninellis and A. De Battisti, *J. Appl. Electrochem.*, in preparation.